Optimal dual-energy computed tomography scan parameters to detect small- sized urinary stones and their composition

Jin-Woo Jung
International St. Mary's Hospital, Catholic Kwandong University College of Medicine
Jun-Bong Shin
Kangwon National University Hospital
Hyo-Jun Choi
International St. Mary's Hospital
Seongyong Pak
Siemens Healthineers Ltd
Hyungjin Yang
Korea University Sejong Campus
Byung Il Yoon (yoonbi0948@catholic.ac.kr)
International St. Mary's Hospital, Catholic Kwandong University College of Medicine

Research Article

Keywords: Dual-energy computed tomography, Urinary stone, Uric acid, Non-uric acid

Posted Date: November 30th, 2022

DOI: https://doi.org/10.21203/rs.3.rs-2312174/v1

Additional Declarations: No competing interests reported.

Version of Record: A version of this preprint was published at Urolithiasis on March 18th, 2023. See the published version at https://doi.org/10.1007/s00240-023-01419-5.

Abstract

Objective

To investigate the optimal scanning parameters of dual-energy computed tomography (DECT), which can accurately determine sensitivity (the detectability of urinary stones) and accuracy (the composition matching of urinary stones), and to apply them to clinical trials.

Methods

Fifteen urinary stones were chemically analyzed, and their chemical compositions were considered a reference standard with which we compared the uric acid (UA) and non-UA compositions determined using DECT. The urinary stones were placed inside a bolus and scanned with a dual-source CT scanner under various selected dual-energy conditions (A to X) using various solid water phantom thicknesses. These datasets were analyzed using the Siemens *syngo*.via software tool (integrated into the CT system) for matching the sensitivity and accuracy assessments.

Results

This study showed that 80% of the highest sensitivity (detection of urinary stones) and 92% of the highest accuracy (composition matching of urinary stones) were achieved under condition A (a collimation beam width setting of 2 × 32 mm × 0.6 mm, an automatic exposure control setting of 80/Sn140 peak kilovoltage, and a slice thickness of 0.5/0.5 mm) ($P < 0.05$).

Conclusion

Application of the DECT energy parameters presented in the study will help identify the sensitivity and accuracy of UA and non-UA stone analysis, even in patients with small-sized urinary stones and in conditions difficult for analysis.

Introduction

Medical imaging based on computed tomography (CT) has recently shown rapid development. Dual-energy CT (DECT), which has mainly been used in recent clinical trials, uses two X-ray energies. The first X-ray spectrum distinguishes different elemental compositions with pixel values identical to those in CT images, depending on the mass density of the material. Further attenuation measurements are performed with the second X-ray spectrum to classify various tissue types and contrast agents. This enables the quantification of the mass density of two or three materials in a mixture with known elemental composition [1]. Urological stone diagnosis based on DECT has replaced traditional intravenous pyelography because it can accurately determine the size, location, and composition of urinary stones

[2–9]. Uric acid (UA) stones (in less than 10% of cases) can be lost after a long metabolism and may be dissolved by medical therapy; thus, it is important to analyze stone composition. Urinary tract stone removal surgery or shockwave surgery can cause complications such as kidney bleeding, fibrosis, and hypertension [10]. If UA stones can be distinguished from non-UA stones using DECT testing, unnecessary urinary tract treatment and its accompanied complications may be avoided in some patients.

Most urinary stones contain two or more materials; thus, it is essential to identify, quantify, analyze, and compare their individual components [11, 12]. Several composition analysis techniques, such as X-ray diffraction crystallography, infrared spectroscopy, scanning electron microscopy with energy dispersion, thermogravimetry, polarized microscopy, and wet chemical analysis, have been used to define the standards against which urinary stone composition can be compared using DECT [13]. To date, there are many studies on urinary stone composition (UA or non-UA) using dual energy, but there is no standardized DECT protocol for differentiating between UA and non-UA stones. In this study, the optimal conditions for DECT are studied by analyzing various variables that may affect the distinction between UA and non-UA stones and by investigating sensitivity (the number of urinary stone detections) and accuracy (the composition matching of urinary stones).

Materials And Methods

Urinary stone

In our study, approved by the institutional review board (IS15EISI0026), 15 urinary stones were obtained after consent from 13 patients who underwent urological surgery (Fig. 1). For the phantom experiments, these 15 stones were numbered from 1 to 15. Following these experiments, the stones were sent to an external institute for chemical analysis. According to the chemical analysis results, the stones were classified into the following four types: five UA stones; five calcium oxalate monohydrate stones; four “fusion” stones with a mixture of calcium oxalate monohydrate, apatite, carbonate apatite, and struvite; and one fusion stone with calcium oxalate monohydrate, calcium oxalate dihydrate, and carbonate apatite. Figure 2 shows images of the phantom and bolus used in the study.

Phantom

Solid water phantom (30 cm × 30 cm × 1 cm)

We used a Blue Water Phantom (Standard Imaging Inc.), composed of a water-equivalent material within 1.0% for photons.

Bolus (30 cm × 30 cm × 1 cm)

The bolus used in the study was composed of a tissue-equivalent gel with a density of 1.03 g/cm^3 (Civco).

Equipment

In this study, a Siemens SOMATOM Definition Flash CT scanner and a Siemens *syngo*.via workstation (software version VA30A HF06) were used (Table 1).

Table 1
Specification of the data acquisition system (Siemens SOMATOM Definition Flash CT)

Data acquisition system	Specification
Max. number of slices/rotations	2 x 128
Number of detector rows	2 x 64
Number of detector electronic channels (DAS) utilized for up to 2 x 128 slices/rotation acquisition	2 x 128

Experimental Arrangement

Urinary stone array

In the experimental phase of the study, the urinary stones from the patients who underwent urological surgery were placed in the bolus at uniformly spaced intervals, as shown in Fig. 3. The use of the bolus prevented damage or breakage of the stones.

Phantom size

A solid water phantom was used to prepare three types of phantom arrangements to consider the “patient thickness.” The phantom thickness was adjusted using solid water, and the number of layers was determined according to the height of the phantom. Figure 4 shows the phantom size according to the thickness of the phantom.

DECT conditions

The images of the stones were obtained by varying the dual-energy scanning parameters according to the phantom thickness (Fig. 4). The variable dual-energy scanning parameters included the tube potential (kV), tube current-time product (mAs), collimation beam width (mm), and slice thickness/increment (mm). The fixed scan parameters included the field of view (300 mm), center X (0 mm), center Y (0 mm), slice thickness (mm), increment (mm), reconstruction algorithm, and reconstruction kernel. Measurements with

all of the four scan parameters were repeated five times. Table 2 lists the dual-energy scanning parameters considered in this study.

Twenty-four possible combinations of dual-energy settings and phantom arrangements were performed. In Table 2 and Fig. 4, these conditions are labeled A to X (Table 3). The measurements were repeated five times for each condition, and the mean of the results was determined.

Table 2
Dual energy scanning parameters applied to the phantom studies

Parameter	Setting
Tube potential (kV), Reference mAs : A / B	80/sn140, 419 / 162
Phantom size : CTDIvol /DLP average (mGy)	100/sn140, 210 / 162
Collimation beam width (mm)	Phantom Ⅰ : 8.18 / 261.8
	Phantom Ⅱ : 9.46 / 301.3
	Phantom Ⅲ : 10.7 / 342.0
	2 × 32 mm × 0.6 mm
	2 × 64 mm × 0.6 mm
Slice thickness / increment (mm)	0.5 / 0.5
Tube current-time product (mAs)	1.5 / 1
Field of view (mm)	Auto exposure control (AEC)
Reconstruction algorithm	300
	SAFIRE Strength-3
Reconstruction kernel	Q30f Medium Smooth

CTDIvol, CT dose index; DLP, dose length product

Table 3
Dual energy parameters (A-X) and phantom sizes (Phantom I - height: 10 cm, phantom II - height: 16 cm, and phantom III - height: 22 cm) pertaining to urinary stone CT scan (slice thickness/increment, collimation beam width, tube potential)

DE scan condition	**slice thickness / increment (0.5 / 0.5 mm)**		**slice thickness / increment (1.5 / 1.0 mm)**	
	Collimation beam width (2 x 32 x 0.6 mm)	**Collimation beam width (2 x 64 x 0.6 mm)**	**Collimation beam width (2 x 32 x 0.6 mm)**	**Collimation beam width (2 x 64 x 0.6 mm)**
Tube potential 80/sn140 (Phantom size)	A(**P- I**), I(**P- II**), Q(**P-III**)	B(**P- I**), J(**P- II**), R(**P-III**)	E(**P- I**), M(**P- II**), U(**P-III**)	F(**P- I**), N(**P- II**), V(**P-III**)
Tube potential 100/sn140 (Phantom size)	C(**P- I**), K(**P- II**), S(**P-III**)	D(**P- I**), L(**P- II**), T(**P-III**)	G(**P- I**), O(**P- II**), W(**P-III**)	H(**P- I**), P(**P- II**), X(**P-III**)

Phantom image analysis

We used a Siemens *syngo.*via workstation to analyze the acquired urinary stone image. This application detects urinary stones and visualizes the chemical differences between them according to the decomposition of the stones into their components: tissue, uric acid, and oxalate (calcium stone). The main advantages of this application are the presence of suitable tools for analyzing urinary stones, easy navigation through the tools, and a rapid evaluation of the urinary stones. The application provides mixed images, fused images, and iodine overlay images. The screenshot of the urinary stone parameter shown in the lower right panel of Fig. 5 provides information such as the volumes of all stones displayed, urinary stone markers, and reference points for typical stones. The multiplanar reconstruction axial color-coded image corresponding to the urinary stone analysis image is shown in Fig. 5C, where the red dotted lines indicate UA stones, and the blue dotted lines indicate calcium stones. As can be seen in the urinary stone parameter diagram shown in Fig. 5D, the UA and non-UA stones are distinguished above and below the baseline (white line).

Statistical method

Sensitivity, accuracy, and comprehensive urinary analysis assessments were done with paired T-test. The paired T-test revealed a significant difference at the 95% confidence level. Significance was set at $P < 0.05$. All statistical tests were performed using SPSS (v22.0.0.0)

Results

Stone analysis report

We commissioned the Seegene Medical Foundation for the chemical analysis of the urinary stones following the DECT-based phantom study. Table 4 shows the results of the chemical analysis provided by the foundation.

Table 4
Results of the urinary stone analysis

Stone No.	Weight (mg)	Diameter (mm)		Composition ingredient (ratio: %)				
				Uric acid	Calcium oxalate monohydrate	Carbonate apatite	Calcium oxalate dihydrate	Struvite
1	23.8	3.5	3	100%				
2	1.8	1.5	0.5		50%	25%		25%
3	15.1	2.5	2		100%			
4	7.1	2	1.5		80%	10%		10%
5	2.5	1.5	1.5	100%				
6	32.6	4.5	2.5	100%				
7	27.8	4.5	2.5	100%				
8	5.9	3	2		100%			
9	1	2	1		100%			
10	6.3	2.5	2		50%	25%	25%	
11	6.4	2	1.5	100%				
12	8.1	2.5	1.5		100%			
13	4.1	2	2		100%			
14	42.9	4.5	3.5		80%	10%		10%
15	31.3	3.5	3		40%	20%		40%

Analysis Results Of The Phantom Study

We compare the analytical results obtained according to the DECT scan conditions (Table 3) with the chemical analysis results (Table 4) to confirm sensitivity and accuracy.

Urinary stone sensitivity

Figure 6 and Table 5 show the results of the urinary stone sensitivity analysis for various dual energy settings and phantom thicknesses. As the phantom thickness increased under constant conditions, the urinary stone sensitivity decreased significantly, while there was no significant difference according to the change in collimation beam width. Differences were only shown in conditions A and B in Phantom I, and conditions U and V in Phantom III. In addition, while there was no significant difference according to the tube potential, there was a difference only in conditions A and B in phantom I under the same conditions. However, the sensitivity of DECT for detection of urinary stones under the same conditions was significantly higher when a 0.5/0.5 mm slice thickness/increment was used compared with a 1.5/1.0 mm thickness ($P < 0.05$). The sensitivity of DECT to detect urinary stones under all given scan conditions was highest under condition A (a collimation beam width setting of 2 × 32 mm × 0.6 mm, an auto exposure control setting of 80/Sn140 peak kilovoltage, and a slice thickness of 0.5/0.5 mm) ($P < 0.05$).

Table 5

Comprehensive results with the percentage corresponding to the sensitivity (detectability) and accuracy (composition analysis matching) of the urinary stones for various dual-energy (DE) scan parameters (A-X) and phantom size (Phantom I - height: 10 cm, phantom II - height: 16 cm, and phantom III - height: 22 cm)

DE scan condition	**slice thickness / increment (0.5 / 0.5 mm)**		**slice thickness / increment (1.5 / 1.0 mm)**	
	Collimation beam width (2 x 32 x 0.6 mm)	**Collimation beam width (2 x 64 x 0.6 mm)**	**Collimation beam width (2 x 32 x 0.6 mm)**	**Collimation beam width (2 x 64 x 0.6 mm)**
Tube potential 80/sn140 (Phantom size) **- Sensitivity (%) & Accuracy (%)**	A(**P- I**) – **80%, 92%**	B(**P- I**) – **73%, 90%**	E(**P- I**) – **67%, 91%**	F(**P- I**) – **67%, 89%**
	I(**P- II**) – **73%, 91%**	J(**P- II**) – **73%, 90%**	M(**P- II**) – **67%, 91%**	N(**P- II**) – **67%, 90%**
	Q(**P-III**) – **73%, 91%**	R(**P-III**) – **73%, 86%**	U(**P-III**) – **53%, 91%**	V(**P-III**) – **47%, 88%**
Tube potential 100/sn140 (Phantom size) **- Sensitivity (%) & Accuracy (%)**	C(**P- I**) – **73%, 91%**	D(**P- I**) – **73%, 90%**	G(**P- I**) – **60%, 91%**	H(**P- I**) – **67%, 90%**
	K(**P- II**) – **73%, 91%**	L(**P- II**) – **73%, 90%**	O(**P- II**) – **67%, 91%**	P(**P- II**) – **67%, 90%**
	S(**P-III**) – **73%, 91%**	T(**P-III**) – **73%, 86%**	W(**P-III**) – **53%, 91%**	X(**P-III**) – **47%, 86%**

Urinary stone accuracy

Figure 7 and Table 5 show the matching rate of component analysis among the total number of urinary stones that can be analyzed under various dual energy conditions (A to X). As the phantom thickness

increased under the same conditions, as the urinary stone component analysis matching was significantly lowered, and under the same conditions, the collimation beam was better at a width of 2 x 32 x 0.6 mm than at a width of 2 x 64 x 0.6 mm. In addition, there were only significant differences according to the tube potential between conditions A and C under the same conditions, conditions F and H under the same conditions, and conditions V and X under the conditions F and H under the phantom III. However, under the same conditions, there was no significant difference in the urea component analysis matching ability of DECT according to the slice thickness/increase. The ability to analyze and match urinary tract stones under the scan conditions of all DECTs was the most likely using condition A (a collimation beam width setting of 2 × 32 mm × 0.6 mm, an auto exposure control setting of 80/Sn140, and a peak thickness of 0.5 < 0.5 mm).

Discussion

In previous studies, DECT scans of medium and large phantoms showed good results (100% accuracy, 40/40) by measuring the accuracy and sensitivity of urinary stones according to the setting of the collimating beam width, proving that the clinical use of urinary stones using DECT is possible [3]. In particular, small stone syndromes can cause sufficient pain with urinary stones measuring 3 mm (range 1.5–4.0 mm) compared to that generally caused by urinary tract obstruction; hence, it is important to detect small urinary stones [14]. Their detection using DECT can help radiologists or urologists to identify diseases. New CT technologies have enabled increasingly accurate analyses of urinary stones with the application of tin filters combined with high-energy tubes and wider energy ranges [15, 16].

According to the DECT-based diagnosis and analysis of urinary stones, UA stones consist of light chemical elements (H, C, N, and O), whereas non-UA stones consist of heavy chemical elements (P, Ca, and S), resulting in very different X-ray attenuating properties at high and low peak kilovoltage (kVp). UA stones have higher CT numbers at higher kVp values, whereas non-UA stones have higher CT numbers at lower kVp values [6]. Consequently, the difference between CT numbers at high and low kVp values can be used to improve the prediction accuracy of the CT number approach [17–19]. Furthermore, current third-generation dual-source CT devices are equipped with selective annotation filters for high-energy X-ray tubes to absorb low-energy photons [20, 21].

Slice thickness is an important scanning parameter under the same CT energy conditions. A thinner slice provides better spatial resolution. Conversely, the noise in CT images increases with a decrease in the thickness of the slices. However, because the sensitivity of the urinary stones depends on the detail and spatial resolution, reducing the slice thickness is expected to achieve better sensitivity. The performance of the dual-energy technique for extra-large-sized patients is limited by two factors. Firstly, the 80-kVp images become extremely noisy, increasing the error bars of the data points representing the stones on the dual-energy plot. The second factor is beam hardening, which is more evident in case of extra-large patients [6]. Thus, the larger the phantom size, the lower the accuracy.

We used the reconstruction kernel setting (e.g., SAFIRE kernel strength) and automatic exposure control (AEC), which are currently used in abdominal examinations in clinical trials and investigated the changes in CT parameters that can affect urinary stone analysis. Conditions A in Phantom I, conditions I and K in Phantom II, and conditions Q and S in Phantom III showed the highest sensitivity and highest accuracy. The most common settings for conditions A, I, K, Q, and S are small collimation beam widths (2 × 32 × 0.6 mm) and small slice thicknesses/increments (0.5/0.5 mm). Considering the previously mentioned results, the most accurate urea analysis results were achieved at small slice thickness/increment values. Therefore, a combination of DECT parameters with a tube potential of 80/sn140, collection beam width of 2 x 32 x 0.6 mm, and slice thickness/increment of 0.5 / 0.5 mm may be providing the highest sensitivity and the highest accuracy for small urinary stones, regardless of patient size.

In previous studies, DECT scanning of medium and large phantoms showed good results (100% accuracy, 40/40) by measuring the accuracy and sensitivity of urinary stones according to the collimation beam width setting [3]. Similarly, in our study, a collimation beam width setting of 2 × 32 mm × 0.6 mm under the same condition was better in determining both the sensitivity and accuracy of urinary stones than the setting of 2 × 64 mm × 0.6 mm. In addition, previous studies used relatively large stones with a size ranging from 2 to 7 mm; however, this study used a small stone of 1.5 to 4.0 mm, Evaluating the sensitivity and accuracy of small urinary tract stones according to the difference in slice thickness/incremental of the DECT scan parameters may give a different result compared to a similar analysis using large stones.

In general, DECT system vendors recommend a slice thickness between 1 mm and 2 mm, which is one of the constraints for urinary stone detection, and an overlapping ratio of −30%. However, according to the findings of our study, the best result can be obtained with a slice thickness/increment setting of 0.5/0.5 mm instead of 1.5/1.0 mm ($P < 0.05$). In addition, in the Siemens *syngo*.via application provided by the vendor, the result of the urinary stone parameter diagram analysis can distinguish UA and non-UA by their color code (Fig. 5D). Vendors have also recommended that stones with diameters less than 3.5 mm may be color- coded incorrectly or not detected at all under other non-standard settings. However, in a study conducted with Phantom III assuming obese patients, condition Q (10 with a diameter < 3.5 mm and 5 with a diameter > 3.5 mm) showed a high urological stone sensitivity of about 72% and a high accuracy of 91%. When setting the DECT scan parameters to detect small-sized urinary stones, the slice thickness and increment must be set to a small value to increase the detection sensitivity and accuracy of urinary stones. However, this experiment has the limitation of being an in-vitro study, and in-vivo research on urolithiasis patients is necessary in the future.

Conclusions

The application of DECT energy parameters presented in this study will help identify the sensitivity and accuracy of UA and non-UA stone analysis, even in patients with small-sized urinary stones and in conditions difficult for analysis.

Declarations

Acknowledgments

No funding was received to assist with the preparation of this manuscript.

Author contributions

Conceptualization: [Jung-Jin Woo], [Jun-Bong Shin], [Hyungjin Yang], [Byung Il Yoon];Methodology: [Jung-Jin Woo], [Jun-Bong Shin], [Hyo-Jun Choi], [Seongyong Pak]; Formal analysis and investigation: [Jung-Jin Woo], [Jun-Bong Shin], [Hyo-Jun Choi], [Seongyong Pak]; Writing - original draft preparation: [Jung-Jin Woo], [Jun-Bong Shin]; Writing - review and editing: [Hyungjin Yang], [Byung Il Yoon]; Resources: [Jung-Jin Woo], [Jun-Bong Shin]; Supervision: [Hyungjin Yang], [Byung Il Yoon]

References

1. McCollough CH, Leng S, Yu L, Fletcher JG (2015) Dual- and Multi-Energy CT: Principles, Technical Approaches, and Clinical Applications. Radiology 276(3):637–653. https://doi.org/10.1148/radiol.2015142631
2. Eiber M, Holzapfel K, Frimberger M, Straub M, Schneider H, Rummeny EJ, Dobritz M, Huber A (2012) Targeted dual-energy single-source CT for characterisation of urinary calculi: experimental and clinical experience. Eur Radiol 22(1):251–258. https://doi.org/10.1007/s00330-011-2231-2
3. Li X, Zhao R, Liu B, Yu Y (2013) Gemstone spectral imaging dual-energy computed tomography: a novel technique to determine urinary stone composition. Urology 81(4):727–730. https://doi.org/10.1016/j.urology.2013.01.010
4. Primak AN, Fletcher JG, Vrtiska TJ, Dzyubak OP, Lieske JC, Jackson ME, Williams JC, Jr., McCollough CH (2007) Noninvasive differentiation of uric acid versus non-uric acid kidney stones using dual-energy CT. Acad Radiol 14(12):1441–1447. https://doi.org/10.1016/j.acra.2007.09.016.
5. Stolzmann P, Scheffel H, Rentsch K, Schertler T, Frauenfelder T, Leschka S, Sulser T, Marincek B, Alkadhi H (2008) Dual-energy computed tomography for the differentiation of uric acid stones: ex vivo performance evaluation. Urol Res 36(3–4):133–8. https://doi.org/10.1007/s00240-008-0140-x
6. Graser A, Johnson TR, Bader M, Staehler M, Haseke N, Nikolaou K, Reiser MF, Stief CG, Becker CR (2008) Dual energy CT characterization of urinary calculi: initial in vitro and clinical experience. Invest Radiol 43(2):112–119. https://doi.org/10.1097/RLI.0b013e318157a144
7. Boll DT, Patil NA, Paulson EK, Merkle EM, Simmons WN, Pierre SA, Preminger GM (2009) Renal stone assessment with dual-energy multidetector CT and advanced postprocessing techniques: improved characterization of renal stone composition–pilot study. Radiology 250(3):813–820. https://doi.org/10.1148/radiol.2503080545
8. Eliahou R, Hidas G, Duvdevani M, Sosna J (2010) Determination of renal stone composition with dual-energy computed tomography: an emerging application. Semin Ultrasound CT MR 31(4):315–

320. https://doi.org/10.1053/j.sult.2010.05.002

9. Kulkarni NM, Eisner BH, Pinho DF, Joshi MC, Kambadakone AR, Sahani DV (2013) Determination of renal stone composition in phantom and patients using single-source dual-energy computed tomography. J Comput Assist Tomogr 37(1):37–45. https://doi.org/10.1097/RCT.0b013e3182720f66
10. Evan AP, Willis LR, Lingeman JE, McAteer JA (1998) Renal trauma and the risk of long-term complications in shock wave lithotripsy. Nephron 78(1):1–8. https://doi.org/10.1159/000044874
11. Cappuccio FP, MacGregor GA (1993) The pathogenesis and treatment of kidney stones. N Engl J Med 328(6):444
12. Daudon M, Donsimoni R, Hennequin C, Fellahi S, Le Moel G, Paris M, Troupel S, Lacour B (1995) Sex- and age-related composition of 10 617 calculi analyzed by infrared spectroscopy. Urol Res 23(5):319–326. https://doi.org/10.1007/bf00300021
13. Kasidas GP, Samuell CT, Weir TB (2004) Renal stone analysis: why and how? Ann Clin Biochem 41(Pt 2):91–97. https://doi.org/10.1258/000456304322879962
14. Jura YH, Lahey S, Eisner BH, Dretler SP (2013) Ureteroscopic treatment of patients with small, painful, non-obstructing renal stones: the small stone syndrome. Clin Nephrol 79(1):45–49. https://doi.org/10.5414/cn107637
15. Apfaltrer G, Dutschke A, Baltzer PAT, Schestak C, Özsoy M, Seitz C, Veser J, Petter E, Helbich TH, Ringl H, Apfaltrer P (2020) Substantial radiation dose reduction with consistent image quality using a novel low-dose stone composition protocol. World J Urol 38(11):2971–2979. https://doi.org/10.1007/s00345-020-03082-6
16. Fung GS, Kawamoto S, Matlaga BR, Taguchi K, Zhou X, Fishman EK, Tsui BM (2012) Differentiation of kidney stones using dual-energy CT with and without a tin filter. AJR Am J Roentgenol 198(6):1380–1386. https://doi.org/10.2214/ajr.11.7217
17. Mostafavi MR, Ernst RD, Saltzman B (1998) Accurate determination of chemical composition of urinary calculi by spiral computerized tomography. J Urol 159(3):673–675
18. Bellin MF, Renard-Penna R, Conort P, Bissery A, Meric JB, Daudon M, Mallet A, Richard F, Grenier P (2004) Helical CT evaluation of the chemical composition of urinary tract calculi with a discriminant analysis of CT-attenuation values and density. Eur Radiol 14(11):2134–2140. https://doi.org/10.1007/s00330-004-2365-6
19. Sheir KZ, Mansour O, Madbouly K, Elsobky E, Abdel-Khalek M (2005) Determination of the chemical composition of urinary calculi by noncontrast spiral computerized tomography. Urol Res 33(2):99–104. https://doi.org/10.1007/s00240-004-0454-2
20. Haubenreisser H, Meyer M, Sudarski S, Allmendinger T, Schoenberg SO, Henzler T (2015) Unenhanced third-generation dual-source chest CT using a tin filter for spectral shaping at 100kVp. Eur J Radiol 84(8):1608–1613. https://doi.org/10.1016/j.ejrad.2015.04.018
21. Primak AN, Ramirez Giraldo JC, Liu X, Yu L, McCollough CH (2009) Improved dual-energy material discrimination for dual-source CT by means of additional spectral filtration. Med Phys 36(4):1359–

1369. https://doi.org/10.1118/1.3083567

Figures

Figure 1

Fifteen urinary stones considered in the study (numbered 1-15)

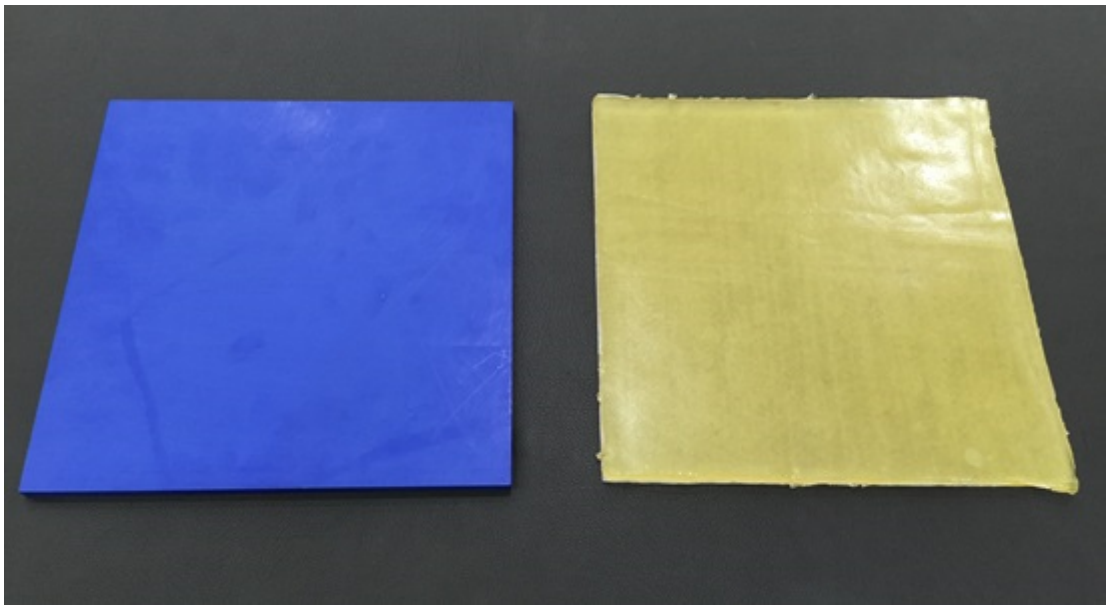

Figure 2

Solid water phantom(left) and bolus(right) used in the study

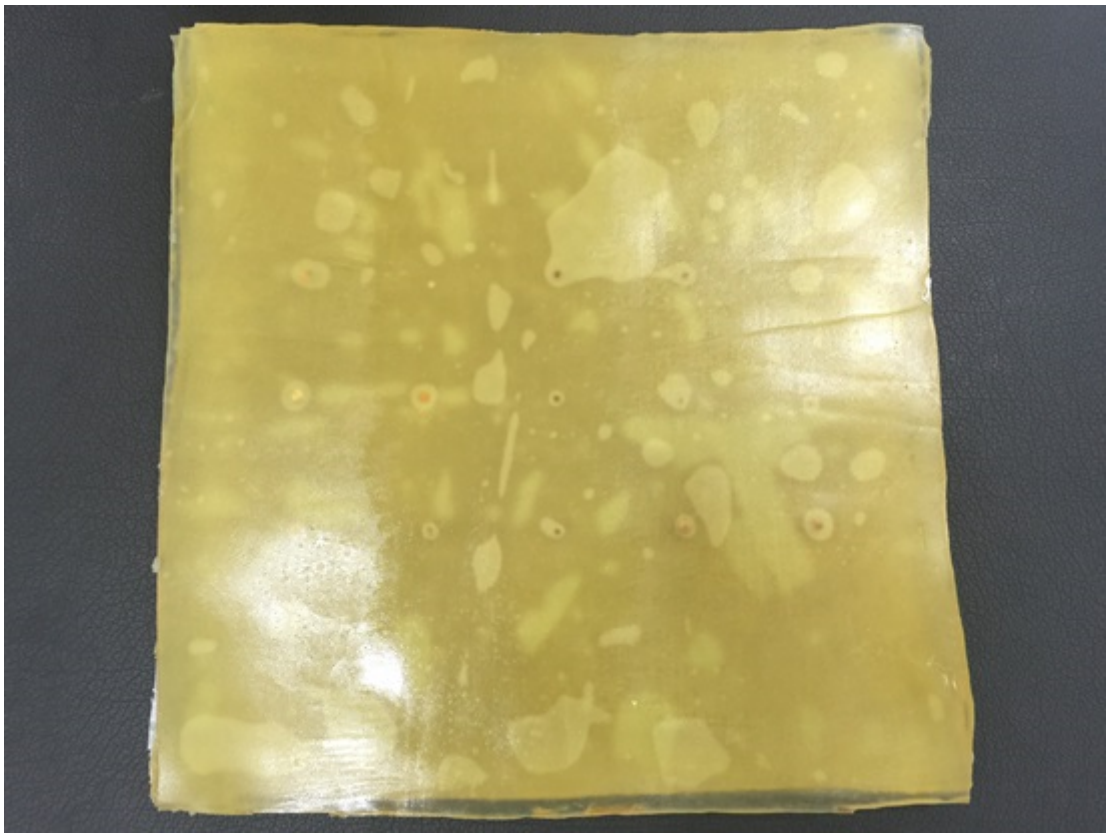

Figure 3

Position of the urinary stones in the bolus (the 15 urinary stones were arranged in three rows, with five stones and a uniform spacing in each row)

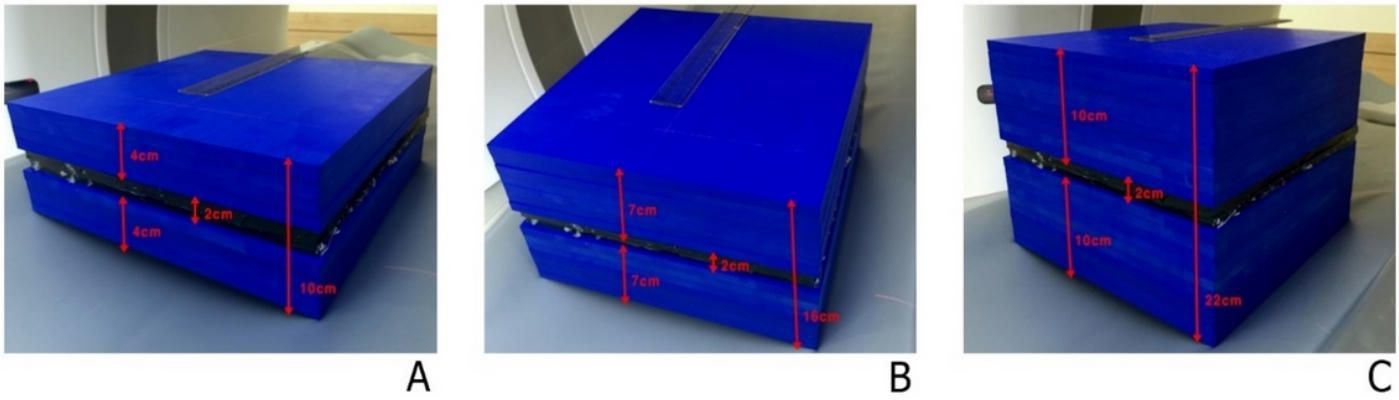

Figure 4

Images of the three phantom arrangements used in the study. (A) Phantom I (height: 10 cm), (B) phantom II (height: 16 cm), and (C) phantom III (height: 22 cm). Each phantom and bolus had a volume of 30 cm × 30 cm × 1 cm

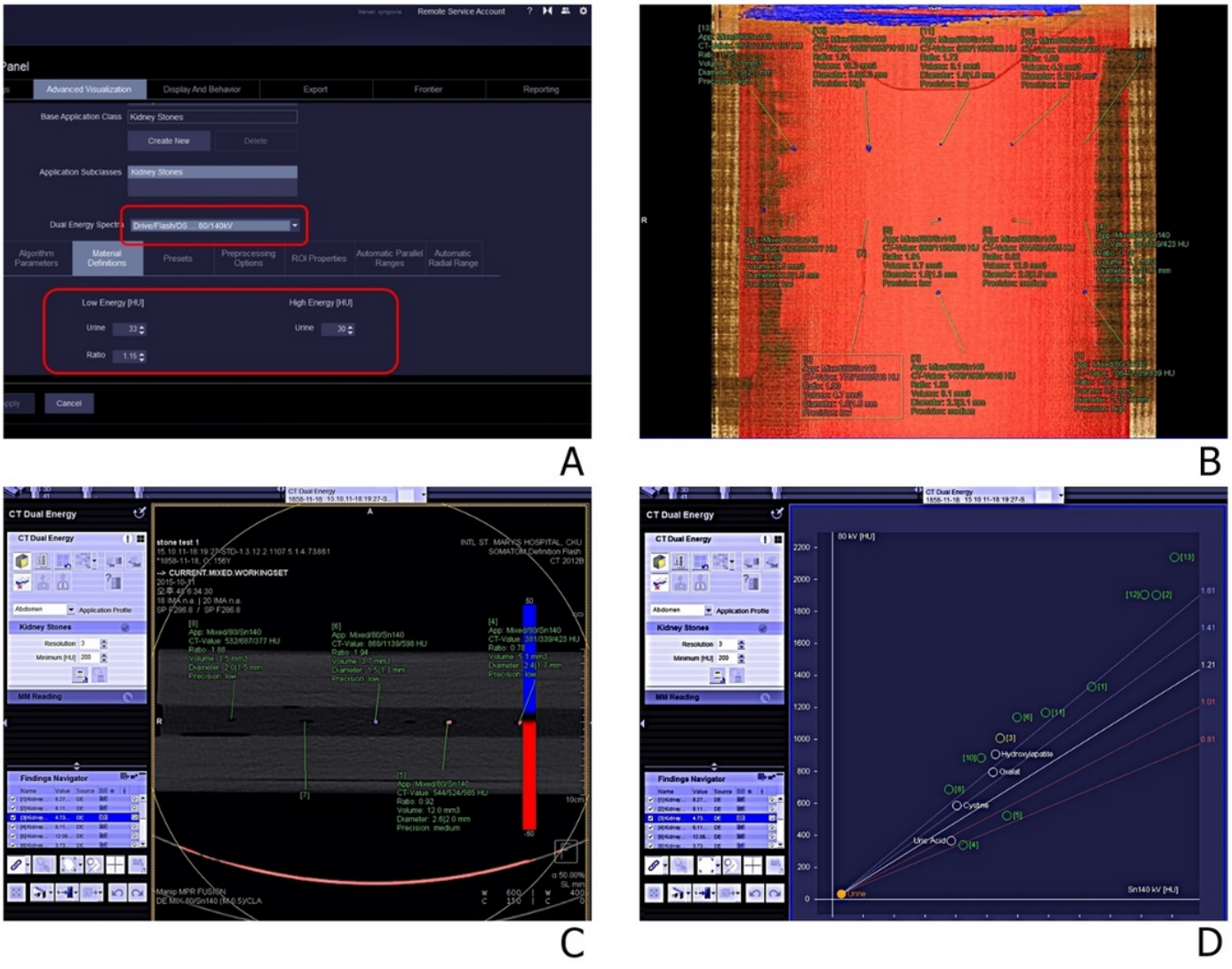

Figure 5

Urinary stone analysis results obtained using Siemens *syngo*.via. (A) Advanced visualization. (B) Multiplanar reconstruction (MPR) coronal color-coded image corresponding to the urinary stone analysis. (C) MPR axial color-coded image corresponding to the urinary stone analysis. (D) Urinary stone parameter diagram

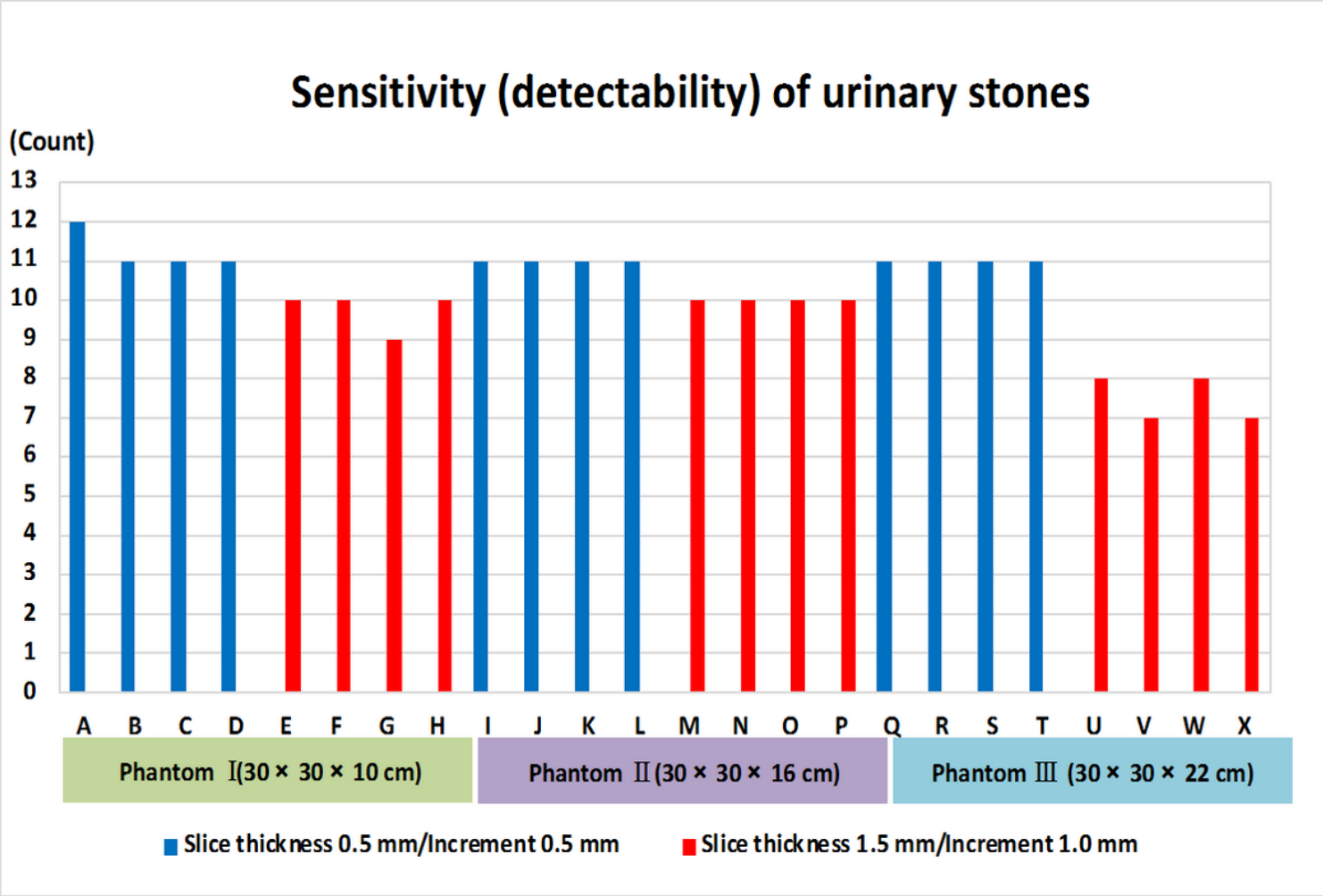

Figure 6

Sensitivity(detectability) of the urinary stone and error value of the urinary stone diameter at various dual-energy conditions (A-X) and phantom thicknesses (-III)

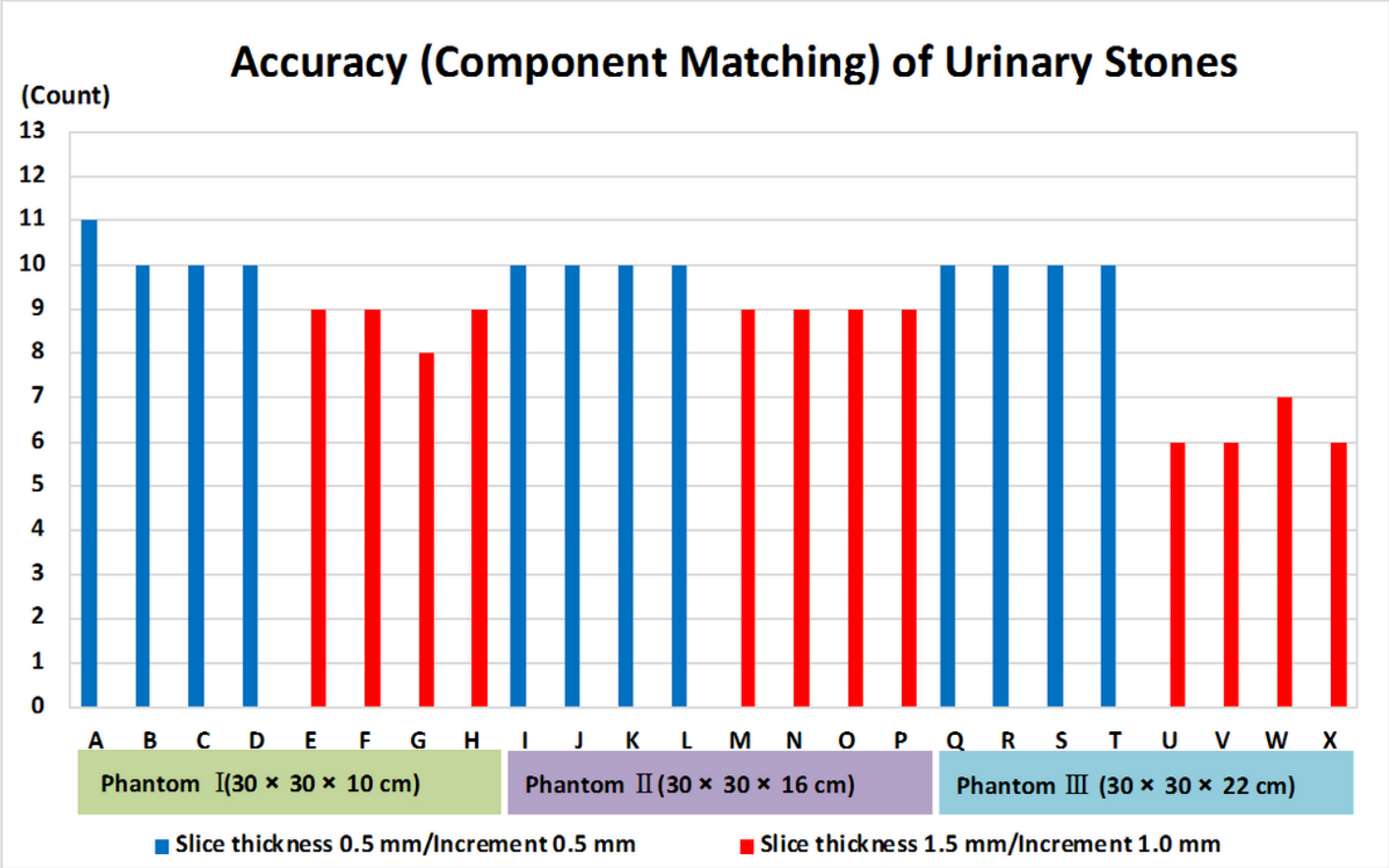

Figure 7

Accuracy (component matching) of the urinary stones at various dual-energy conditions (A-X) and phantom thicknesses (–III)